Systematic pre-annotation explains the "dark matter" in LC-MS metabolomics

Yuanye Chi[1], Joshua M. Mitchell[1], Shujian Zheng[1] and Shuzhao Li[1,2*]

[1]The Jackson Laboratory for Genomic Medicine, 10 Discovery Drive, Farmington, CT 06032, USA

[2]University of Connecticut School of Medicine, Farmington, CT 06032, USA

*Corresponding author, E-mail: shuzhao.li@jax.org

Abstract

The majority of features in global metabolomics from high-resolution mass spectrometry are typically not identified, referred as the "dark matter". Are these features real compounds or junk? Understanding this problem is critical to the annotation and interpretation of metabolomics data and future development of the field. Recent debates also brought attention to in-source fragments, which appear to be prevalent in spectral databases. We report here a systematic analysis of 61 representative public datasets from LC-MS metabolomics, the most common data type in biomedical studies. The results indicate that in-source fragments contribute to less than 10% of features in LC-MS metabolomics. Khipu-based pre-annotation shows that majority of abundant features have identifiable ion patterns. This suggests that the "dark matter" in LC-MS metabolomics is explainable in an abundance dependent manner; most features are from real compounds; the number of compounds is much smaller than that of features; most compounds are yet to be identified.

The "dark matter" of metabolomics refers to the large number of unidentified features in metabolomic studies, mostly from mass spectrometry (MS) based analysis (deSilva2015; Monge2019). The topic is pertinent to the analytical coverage of small molecules in biomedical research (Kind2009; Uppal2016), approaches to metabolite annotation (Domingo2018; Chaleckis2019; Metz2025), mapping reaction pathways (Zamboni2015; Artyukhin2018) and the promise of applying metabolomics and exposomics to precision medicine (Wishart2016; Vermeulen2020; David2021). Multiple factors contribute to this "dark matter". Modern MS brings tremendous new power into chemical analysis, enabling the detection of compounds that were previously elusive due to limited separation, abundance or stability (Xian2012; Uppal2016; Lai2024). Biology has knowledge gaps and new biochemical mechanisms continue to be discovered. E.g. hundreds of unknown metabolites can be affected by one enzyme (Artyukhin2018; Heremans2022). Such results suggest that characteristic metabolite modifications may be as widespread as protein posttranslational modifications. Our cohabitation with the microbiome results in sharing many metabolites from under-characterized microbial species (Peisl2018). Challenges exist in data acquisition, processing and interpretation. Contamination is common in tandem mass spectra (MS/MS) from biological samples (Stancliffe2021). Artifacts can be generated by data processing software when sensitivity is not matched to detection confidence (Li2023b). Because isotopologues, adducts and fragments are commonly measured in the MS data, it is an apt question if the measured metabolome is inflated by degenerate features (Mahieu2017; Wang2019; Li2023a).

In-source fragments (ISFs), generated when molecules are broken down by ionization energy, became a focus of recent debates. Giera et al (2024) reported that ISFs accounted for over 70% of MS/MS features in METLIN, one of the leading spectral databases, suggesting that ISFs could be a significant portion of the "dark matter". El Abiead et al (2025) calculated the presence of ISFs using a different compound library, reporting less percentage but still two fragments on average per protonated compound. However, both studies focused on data from chemical standards, which are primarily used for metabolite annotation. Currently, the majority of metabolomics data in biomedical research are produced using LC-MS (liquid chromatography coupled mass spectrometry). Biological samples are complex: a LC-MS spectrum often contains more than 1000 mass peaks while a MS/MS spectrum of chemical standards has usually less than 100. It is common in LC-MS that over 1000 spectra are collected on one sample during the chromatographic separation. Therefore, feature detection in LC-MS data requires consecutive elution patterns, a quality filter removing many inconsistent data points. The LC-MS data from

biological samples are very different from that of chemical standards. The real number of metabolites and impact of ISFs should be assessed directly on biological data.

Here, we report a systematic analysis of LC-MS metabolomics from 61 representative public datasets. The relationships of isotopologues, adducts and fragments are determined by mass differences between coeluting features, in a process termed "pre-annotation" (Li2023a). Our results indicate that the contribution of ISFs is small in LC-MS metabolomics, but majority of abundant features have identifiable ion patterns. This suggests that the "dark matter" in metabolomics is explainable in an abundance dependent manner.

Results

LC-MS metabolomics data have a long tail of low intensity features

High-resolution mass spectrometers, with electron spray ionization (ESI), are now routinely employed in metabolomics. From public repositories, we retrieved 61 LC-MS metabolomics datasets. These include 45 studies from orbital mass analyzers (Orbitrap) and 16 from time-of-flight (TOF) analyzers, using in positive or negative ionization (**Figure 1a**, **Table S1**). For consistence of data analysis, only studies of human plasma or serum samples are included, and large datasets are down selected to about 100 samples, because low-frequency features accumulate by increasing sample number. We use the asari software (Li2023b) for processing raw data to features of unique m/z (mass-to-charge ratio) and retention time (RT). Asari is designed with explicit data models that report all features above a quality threshold (signal-to-noise ratio, or SNR, of 2, peak shape of 0.5). The median number of reported features in the Orbitrap studies is around 50,000, of which about a quarter to a third are considered high-quality features (SNR > 5, peak shape > 0.9). Because all organic molecular species contain both ^{12}C and ^{13}C (carbon 13, often under detection limit for low-abundance compounds) natural isotopologues, the presence of $^{13}C/^{12}C$ pair indicates high-confidence detection of a compound. The numbers of $^{13}C/^{12}C$ pairs are typically between 2,000 to 3,000 in these metabolomic datasets (**Figure 1b**). Signal intensity in a typical study follows a long-tail distribution, where about 9% features have higher intensity than 1E6 (**Figure 1c**).

Organizing peaks into putative compounds

The number of features is not a direct account of number of compounds, due to the existence of isotopologues, adducts and fragments. The complexity is illustrated for a compound analyzed from its chemical standard and from a biological sample (MS profiles, **Figure 2a**). This compound shows mass peaks for two adducts, two neutral losses of H_2O and three

isotopologues (**Figure 2b**). It is important to note that features of interest in a spectrum are mass peaks, while in the current practice of LC-MS, features are elution peaks that are observed in consecutive spectra (**Figure 2c**). There is a major reduction of data complexity by feature detection in LC-MS; the complexity of redundant features is then reduced by the process of pre-annotation.

We have previously described a software algorithm, khipu, to perform de novo, global pre-annotation (Li2023a, Mitchell2024b). In short, a khipu aligns coeluting ions on a grid (a tree in computer term) of isotopologues and modifications, where modifications include adducts and fragments (**Figure 2d,e**). Conjugates of compounds (multimers) are less common and not included here. If a feature finds no relationship to other ions, it is called a singleton. The khipu construction leads to an inferred neutral mass, and the data structure enables downstream computing. Not all khipus have multiple adducts, but the ^{13}C ion is expected to be present for all organic compounds of reasonable abundance. Therefore, a khipu indicates a bona fide compound (present in the sample, not necessarily of biological origin). The number of khipus is the estimate of number of high-confidence compounds in the data.

Applying this pre-annotation to all datasets reveals that each dataset typically contains 5~6,000 khipus, which explain about 16,000 features in ESI+ or ESI- data (**Figure 2f**). The average khipu contains three features (the compound shown in Figure 2a-e is atypical). These numbers are in line with high-quality features in **Figure 1b**, suggesting that we are close to a full explanation of them. We next compare the neutral mass values of khipus to HMDB (version 5, Wishart2022), the leading metabolite database. On average, about 30% of these khipus are matched to HMDB, indicating the majority of compounds in these studies are unknown (**Figure 2g**).

Common mass differences in LC-MS and application to ISF estimation

The pre-annotation approach depends on the list of mass differences underlying the ion patterns. The khipu software includes default lists of isotopes and adducts based on prior data. To be comprehensive, we also systematically calculated all common mass differences between coeluting features in these current LC-MS datasets (**Table S2-5**). The coelution window here is defined as two standard deviation of RT differences of all $^{13}C/^{12}C$ pairs. Not surprisingly, the m/z difference between $^{13}C/^{12}C$ isotopologues is by far the most frequent observation in both ESI+ and ESI- data (**Figures 3a, S1a**). The top frequent mass differences, excluding known isotopic and adduct patterns, can be considered as candidates for ISFs (also referred as neutral losses).

121 To assess the impact of ISFs on full metabolomic profiles, we compare the pre-annotations
122 without and with consideration of ISFs. Without ISFs, the khipu algorithm is applied to the LC-
123 MS datasets using a conservative set of isotopologues and adducts (**Methods**), to produce a
124 set of khipus and singletons per dataset. The numbers of khipus and singletons can be
125 impacted by ISFs, but ISFs do not impact relationships between isotopologues and adducts.
126 Next, to consider ISFs, the candidate ISFs (**Table S6, Figures 3a, S1a**) are searched between
127 khipus, and between singletons and khipus. The comparison between two steps reveals that in
128 the ESI+ data, about 500 khipus and 700 singletons can be explained by the candidate ISFs
129 (**Figure 3b**), which correspond to about 8% of khipus and 1% of all features, respectively
130 (**Figure 3c**). In the ESI- data, the candidate ISFs explain about 5% of khipus and 1% of extra
131 features (**Figure 3b,c**). While these results do not rule out additional ISFs among singleton
132 features, singletons are of lower intensity and expected to contain even less percentage of
133 fragments.

134 The above approach is an approximation. Examining the RT shift of these candidate ISFs
135 shows that the majority have identical RT as their molecular ions, confirming coelution in
136 chromatography (**Figure S1b**). The RT shift distributions in **Figure s1b** bear two shoulder
137 peaks, which suggest that a subset of matched ISFs is not truly coeluting, thus not fragments
138 but different compounds. This can lead to overestimation in **Figure 3b,c**. The candidate ISFs
139 are not exhaustive, not considering chemical structures in their preference of fragmentation,
140 which could lead to minor underestimation. We next investigate ISFs using a different approach
141 via MS/MS spectra.

142 **MS/MS based search also shows less than 10% ISFs in LC-MS data**

143 Typically, ESI is used in MS to avoid breaking up the molecules. In contrast, MS/MS techniques
144 fragment molecules intentionally by a collision energy, and the fragments serve as a fingerprint
145 of the molecule. If ISFs of a molecule are present in LC-MS data, they must a) have the same
146 retention time as the intact molecules, and b) have m/z values that are similar to those in the
147 corresponding MS/MS spectra. In Giera et al (2024), MS/MS data at zero collision energy were
148 used to mimic MS data. We take a similar strategy here to compare an MS/MS database
149 (MoNA2024) to the LC-MS metabolomics data, requiring both the precursor and at least one
150 MS/MS fragment to be observed in MS data (**Figure 4a**). Even though MoNA database does
151 not fully cover the LC-MS metabolomics data, the number of matched MS/MS fragments relative
152 to the matched precursor ions should indicate the prevalence of ISFs. We parsed out 13,672
153 compounds from MoNA MS/MS spectra. They typically match to 5~10,000 features by

precursor m/z values (**Figure 4b**). Of these matched precursor ions, about 7% have at least one matched MS/MS fragment in the elution window for positive ESI data, about 5% for negative ESI (**Figure 4c**). These results confirm the above khipu analysis that ISFs impact less than 10% of LC-MS features. The results are expected to include false positives (thus overestimation), as a) MS/MS fragments generated by higher collision energies are not expected to be in the LC-MS data; and b) matched features are not necessarily generated by ISF.

An abundance dependent explanation of the "dark matter "

While the numbers of features explained by khipus are given in **Figure 2f**, we are reminded that high-abundance features are a small fraction of all data (**Figure 1c**). To test the dependency of pre-annotation on feature abundance, we split the features in each dataset by intensity into quartiles and visualize the pre-annotation for each quartile. The results show that about 60% of features in the top quartiles are explained by khipus in ESI+ or ESI- data, while the pre-annotated percentage is smaller in lower quartiles (**Figure 5a**). Within the top quartile, the singletons, i.e., features not explained by khipus, have significantly lower intensity than M0 features (**Figure 5b**), corroborating the observation that pre-annotation is bound by abundance. Plotting the result using full quantile range returns a similar conclusion, where pre-annotation reaches 80% at the top end of quantiles (**Figure 5c**). The analysis using 16 studies on time-of-flight platforms returned similar results (**Tables S1**, **S7**). To test the impact of peak alignment on the results, we selected one random sample (thus avoiding peak alignment) from each dataset to repeat the full data processing and pre-annotation, which returned similar results (not shown).

Discussion

In summary, we have carried out systematic pre-annotation on 61 LC-MS metabolomics datasets, representing a reasonable survey of the current data landscape. The results from two different approaches indicate that less than 10% of features in LC-MS are explained by ISFs, while the number may vary between studies. On the surface, this is quite different from the numbers reported by Giera et al (2024) and El Abiead et al (2025). However, results from all three studies have a consistent explanation. ESI can generate many fragments but of low intensity (also pointed out by El Abiead et al, 2025). In the analysis of authentic chemical standards, many ISFs are detected by mass spectrometer because there is little background, while the percentage varies by platforms. There are often over 1 million mass peaks per sample in LC-MS metabolomics, where data are processed into features based on elution peaks. Most ISFs are not observed in LC-MS feature detection because a) signals inconsistent cross scans

are filtered out by elution peaks, and b) low intensity ISFs are outcompeted by more abundant molecular species in the complex matrix of biological samples.

Is the metabolomics "dark matter" real metabolites or junk? The majority of abundant features in LC-MS are already explained by the khipu-based pre-annotation. This indicates that the interpretation of less abundant features is just limited by concentration and ionization efficiency. Therefore, the "dark matter" of metabolomics is largely explainable and should not be considered as mystery. The corollary is that the overwhelming majority of LC-MS metabolomic features from human blood samples are of real compounds. The number of compounds is much smaller than the number of features. Most of these compounds are not matched in HMDB and considered unknown. We do not assume all the compounds are of biological origin. A compound should only be considered as a biological metabolite based on evidence of its activity.

Several precautions may protect us from confusions in the field. Metabolomics moves the traditional analytical chemistry to the -omics scale of complex data. Statistics in spectral databases is difficult to extrapolate directly into LC-MS metabolomics on biological samples. Explicit data models are important to define the purpose and context of results; and analyzing complex data calls for reusable software tools and code (Mitchell2024a). There are many data points and low-quality features in metabolomics data, easily leading to artifacts in computational processing (Li2023b). Different from calling nucleotide bases in genomics, metabolomics features are analog signals that require explicit quality metrics. There are clear benefits to separate pre-annotation from annotation. In genomics, a gene sequence can be deposited for many years before annotation is assigned. While the metabolomics community continues working on compound identification, pre-annotation already answers import questions. The inflation of compound numbers in database searches can be much reduced by using neutral mass from pre-annotation, not individual m/z features.

The size of metabolome depends on the depth and coverage of analysis. Detection frequency across samples also varies greatly on compounds, raising the question of distinguishing metabolome from exposome (Banbury2025). This study does not address how the coverage of different datasets is affected by experimental methods and conditions, which should be a focus of future computational data processing and annotation.

Data and Code Availability:

All asari processed data are available at: https://zenodo.org/records/14541717. The lists of mass patterns for isotopologues, adducts and ISFs are included in the mass2chem software package, freely available at https://github.com/shuzhao-li-lab/mass2chem. All data analysis in this work is provided as Jupyter notebooks at https://github.com/shuzhao-li-lab/in_source_fragments_serum.

Author Contributions

Project design and writing: SL. Data collection and processing: YC. In-house spectra acquisition: SZ. Data analysis: SL, YC. Software development: JM, YC, SL. All authors participated in and approved the final manuscript.

Acknowledgements

This work was in part supported by NIH grant R01 AI149746 (NIAID) and ARPA-H award D24AC00345.

233 **Supplemental Information**

234

235 Table S1. List of datasets used in this work, including 45 Orbitrap studies and 16 TOF studies.

236 Table S2. Most frequent mass differences in Orbitrap ESI+ data.

237 Table S3. Most frequent mass differences in Orbitrap ESI- data.

238 Table S4. Most frequent mass differences in TOF ESI+ data.

239 Table S5. Most frequent mass differences in TOF ESI- data.

240 Table S6. Isotopologues, adducts and ISFs used for extended khipu search.

241 Table S7. Results of features explained in TOF LC-MS metabolomics data.

242

243 Figure S1. Additional common mass differences and distribution of retention shift.

244

245

References

Artyukhin, A.B., Zhang, Y.K., Akagi, A.E., Panda, O., Sternberg, P.W. and Schroeder, F.C., 2018. Metabolomic “dark matter” dependent on peroxisomal β-oxidation in Caenorhabditis elegans. *Journal of the American Chemical Society*, *140*(8), pp.2841-2852.

Banbury Exposomics Consortium. 2025. Integrating Exposomics into the Biomedical Enterprise. Science. In press.

Chaleckis, R., Meister, I., Zhang, P. and Wheelock, C.E., 2019. Challenges, progress and promises of metabolite annotation for LC–MS-based metabolomics. *Current opinion in biotechnology*, *55*, pp.44-50.

David, A., Chaker, J., Price, E.J., Bessonneau, V., Chetwynd, A.J., Vitale, C.M., Klánová, J., Walker, D.I., Antignac, J.P., Barouki, R. and Miller, G.W., 2021. Towards a comprehensive characterisation of the human internal chemical exposome: Challenges and perspectives. *Environment International*, *156*, p.106630.

Domingo-Almenara, X., Montenegro-Burke, J.R., Benton, H.P. and Siuzdak, G., 2018. Annotation: a computational solution for streamlining metabolomics analysis. *Analytical chemistry*, *90*(1), p.480.

El Abiead, Y., Rutz, A., Zuffa, S., Amer, B., Xing, S., Brungs, C., Schmid, R., Correia, M.S., Caraballo-Rodriguez, A.M., Zarrinpar, A. and Mannochio-Russo, H., 2025. Discovery of metabolites prevails amid in-source fragmentation. *Nature Metabolism*, pp.1-3.

Giera, M., Aisporna, A., Uritboonthai, W. and Siuzdak, G., 2024. The hidden impact of in-source fragmentation in metabolic and chemical mass spectrometry data interpretation. *Nature metabolism*, pp.1-2.

Heremans, I.P., Caligiore, F., Gerin, I., Bury, M., Lutz, M., Graff, J., Stroobant, V., Vertommen, D., Teleman, A.A., Van Schaftingen, E. and Bommer, G.T., 2022. Parkinson's disease protein PARK7 prevents metabolite and protein damage caused by a glycolytic metabolite. *Proceedings of the National Academy of Sciences*, *119*(4), p.e2111338119.

Huber, F., van der Hooft, J. J. J., Spaaks, J. H., Diblen, F., Verhoeven, S., Geng, C., Meijer, C., Rogers, S., Belloum, A., Spreeuw, H., Villanueva Castilla, E. M., Ashouritaklimi, K., de Jonge, N., Hecht, H., Skoryk, M., Ahmad, Z., Aleksander Piciga, Rutz, A., & Pollmann, J. (2024). matchms (0.27.0). Zenodo. https://doi.org/10.5281/zenodo.12706344

Kind, T., Scholz, M. and Fiehn, O., 2009. How large is the metabolome? A critical analysis of data exchange practices in chemistry. *PloS one*, *4*(5), p.e5440.

Lai, Y., Koelmel, J.P., Walker, D.I., Price, E.J., Papazian, S., Manz, K.E., Castilla-Fernández, D., Bowden, J.A., Nikiforov, V., David, A. and Bessonneau, V., 2024. High-resolution mass spectrometry for human exposomics: Expanding chemical space coverage. *Environmental Science & Technology*, *58*(29), pp.12784-12822.

Li, S., Siddiqa, A., Thapa, M., Chi, Y. and Zheng, S., 2023b. Trackable and scalable LC-MS metabolomics data processing using asari. *Nature Communications*, *14*(1), p.4113.

Li, S. and Zheng, S., 2023a. Generalized tree structure to annotate untargeted metabolomics and stable isotope tracing data. *Analytical chemistry*, *95*(15), pp.6212-6217.

Mahieu, N. G.; Patti, G. J., Systems-Level Annotation of a Metabolomics Data Set Reduces 25 000 Features to Fewer than 1000 Unique Metabolites. *Anal Chem* **2017,** *89* (19), 10397-10406.

MassBank of North America (MoNA) [retrieved Feb 8, 2024]; Available from: https://mona.fiehnlab.ucdavis.edu/.

Mitchell, J.M., Chi, Y., Thapa, M., Pang, Z., Xia, J. and Li, S., 2024a. Common data models to streamline metabolomics processing and annotation, and implementation in a Python pipeline. *PLOS Computational Biology*, *20*(6), p.e1011912.

Mitchell, J.M., Chi, Y., Zheng, S., Thapa, M., Wang, E. and Li, S., 2024b. Annotation of Metabolites in Stable Isotope Tracing Untargeted Metabolomics via Khipu-web. *Journal of the American Society for Mass Spectrometry*, *35*(12), pp.2824-2835.

Monge, M.E., Dodds, J.N., Baker, E.S., Edison, A.S. and Fernández, F.M., 2019. Challenges in identifying the dark molecules of life. *Annual Review of Analytical Chemistry*, *12*(1), pp.177-199.

Peisl, L., Schymanski, E.L. and Wilmes, P., 2018. Dark matter in host-microbiome metabolomics: tackling the unknowns–a review. *Analytica Chimica Acta*, *1037*, pp.13-27.

Stancliffe, E., Schwaiger-Haber, M., Sindelar, M. and Patti, G.J., 2021. DecoID improves identification rates in metabolomics through database-assisted MS/MS deconvolution. *Nature methods*, *18*(7), pp.779-787.

Uppal, K., Walker, D.I., Liu, K., Li, S., Go, Y.M. and Jones, D.P., 2016. Computational metabolomics: a framework for the million metabolome. *Chemical research in toxicology*, *29*(12), pp.1956-1975.

Vermeulen, R., Schymanski, E.L., Barabási, A.L. and Miller, G.W., 2020. The exposome and health: Where chemistry meets biology. *Science*, *367*(6476), pp.392-396.

Wang, L.; Xing, X.; Chen, L.; Yang, L.; Su, X.; Rabitz, H.; Lu, W.; Rabinowitz, J. D., Peak Annotation and Verification Engine for Untargeted LC-MS Metabolomics. *Anal Chem* **2019,** *91* (3), 1838-1846.

Wishart, D.S., 2016. Emerging applications of metabolomics in drug discovery and precision medicine. *Nature reviews Drug discovery*, *15*(7), pp.473-484.

Wishart, D.S., Guo, A., Oler, E., Wang, F., Anjum, A., Peters, H., Dizon, R., Sayeeda, Z., Tian, S., Lee, B.L. and Berjanskii, M., 2022. HMDB 5.0: the human metabolome database for 2022. *Nucleic acids research*, *50*(D1), pp.D622-D631.

Xian, F., Hendrickson, C.L. and Marshall, A.G., 2012. High resolution mass spectrometry. *Analytical chemistry*, *84*(2), pp.708-719.

346 Zamboni, N., Saghatelian, A. and Patti, G.J., 2015. Defining the metabolome: size, flux, and
347 regulation. *Molecular cell*, *58*(4), pp.699-706.
348

349

350 **Figures**

351 **Figure 1. Processing and analysis of 61 LC-MS studies**

352 **a**. Schematic of pre-annotation analysis, from orbital or time-of-flight instruments. ESI: electron
353 spray ionization; ISF: in-source fragment. M0: the isotopic form of ^{12}C only. The results from 16
354 TOF datasets are shown in supplements.

355 **b.** Across the 22 Orbitrap studies using positive ionization, the median number of features is
356 50,771, the median number of good features 18,117, and the number of matched $^{13}C/^{12}C$ pairs
357 2,176. Similar numbers are observed across the 23 negative ionization Orbitrap studies with
358 48,212 features, 11,783 good features, and 3,008 $^{13}C/^{12}C$ pairs. Good features are defined as
359 having SNR > 5 and peak shape > 0.9 when fitting to a gaussian curve.

360 **c**. Long-tail distribution of feature intensity, where intensity is plotted at log10 scale. Example
361 from dataset ST002200_RPpos_17min_B3_ppm5_3422144, total 50,647 features. Insert
362 boxplot is the fraction of features above 1E6 in intensity, cross 22 Orbitrap ESI+ datasets.

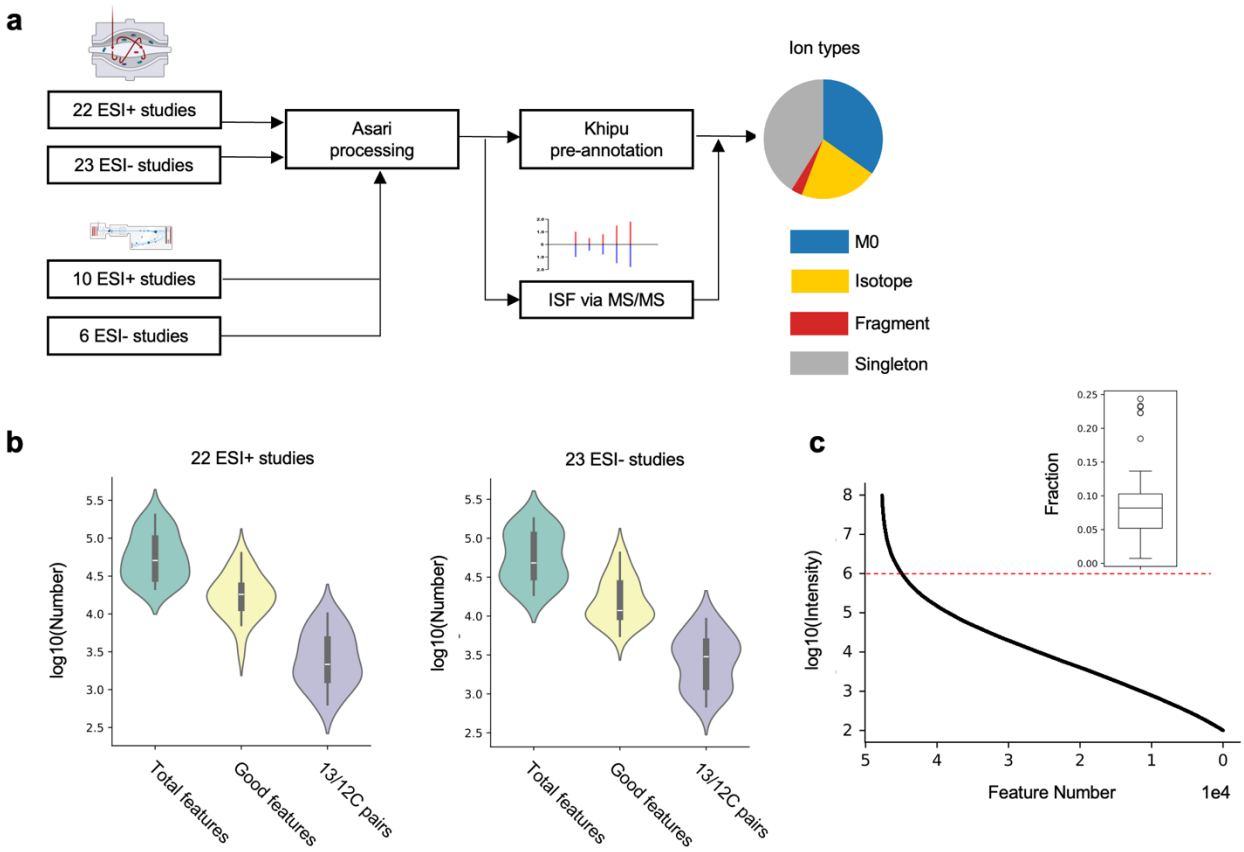
a
22 ESI+ studies
23 ESI- studies
10 ESI+ studies
6 ESI- studies
Asari processing
Khipu pre-annotation
ISF via MS/MS
Ion types
M0
Isotope
Fragment
Singleton
b
22 ESI+ studies
23 ESI- studies
log10(Number)
Total features
Good features
13/12C pairs
c
log10(Intensity)
Feature Number
1e4
Fraction

363

364 **Figure 2: LC-MS metabolomics features explained by khipu pre-annotation.**

365 **a**. Full scan mass spectra of glycochenodeoxycholic acid, analyzed from chemical standard
366 (top, containing impurities) and observed in a biological sample (bottom. Sample 214 in study
367 ST002112_RPpos_B3_ppm5_356194, RT 619.49 second). This is chosen to illustrate a
368 complex ion pattern, while most metabolites have fewer ions. MS/MS data can be generated on
369 a mass peak here, but are not included in this figure.

370 **b.** Manual interpretation of the mass peaks (red in **a**). Smaller peaks of the same color are M2
371 and M3 isotopologues, which are difficult to see in the full mass range in **a**.

372 **c.** Example mass tracks (extracted ion chromatogram) from same biological sample. Elution
373 profiles are composed from consecutive spectra (scan numbers 600-650), each dot from one
374 spectrum. Red box marks the LC-MS features related to glycochenodeoxycholic acid. Reported
375 retention time may be adjusted by alignment cross samples.

376 **d**. Example of khipu pre-annotation of isotopologues, adducts and fragments in a tree structure,
377 with m/z values labeled for each ion.

378 **e.** Khipugram visualization of the data in **d**. Khipu is both the name of software and of a group of
379 ions belonging a putative compound.

380 **f**. Numbers of pre-annotated features cross studies, median value 16,574 and 16,296 for
381 positive and negative ionization datasets, respectively. They correspond to 5,539 and 5,937
382 unique khipus, of which 1866 and 1692 matched to HMDB version 5 by neutral mass,
383 respectively.

384 **g.** Average matches of khipus to HMDB are 31.8% and 28.6%, for positive and negative
385 ionization datasets, respectively.

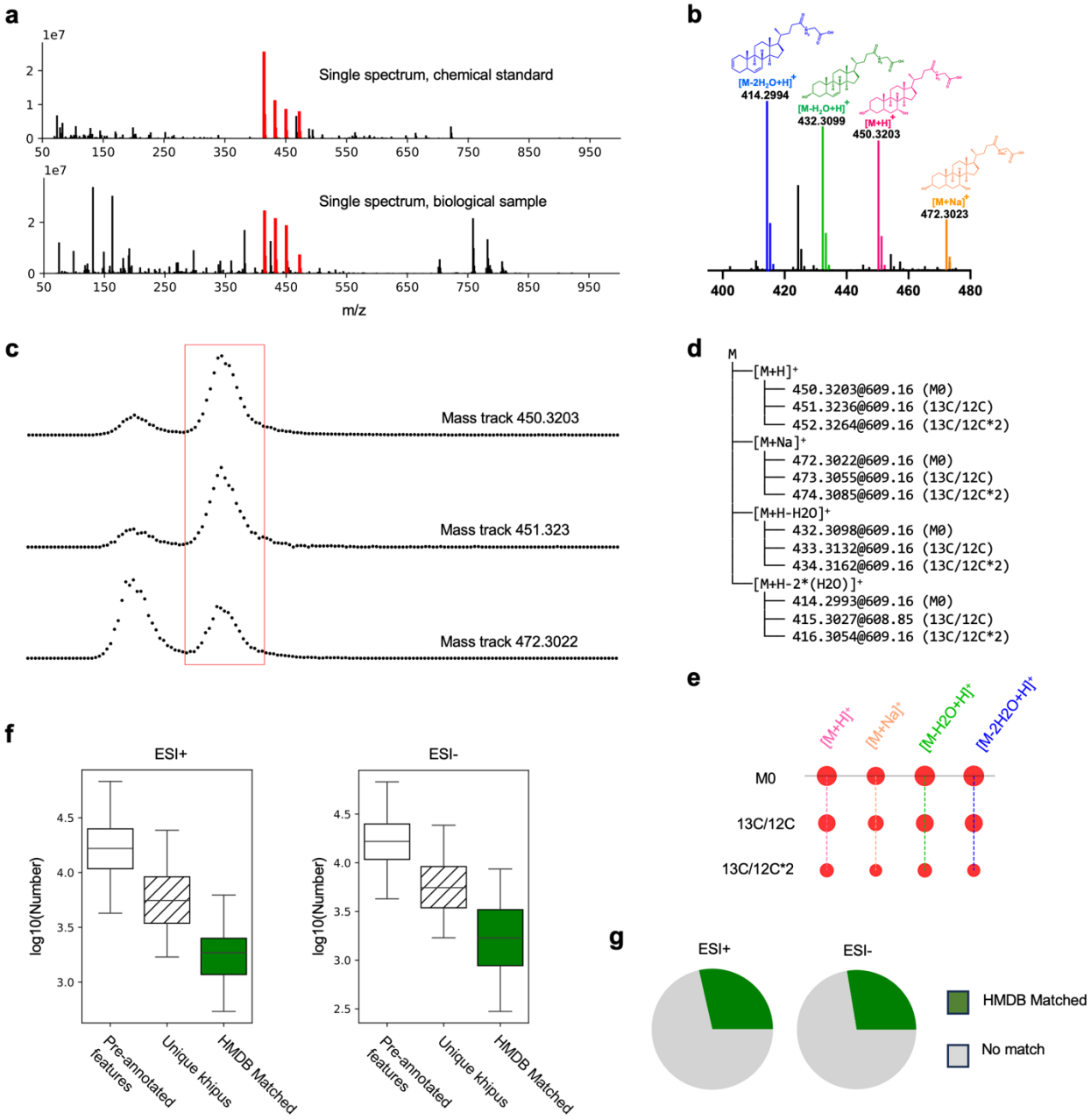
a
1e7
Single spectrum, chemical standard
Single spectrum, biological sample
m/z
b
[M-2H2O+H]+
414.2994
[M-H2O+H]+
432.3099
[M+H]+
450.3203
[M+Na]+
472.3023
c
Mass track 450.3203
Mass track 451.323
Mass track 472.3022
d
M
[M+H]+
450.3203@609.16 (M0)
451.3236@609.16 (13C/12C)
452.3264@609.16 (13C/12C*2)
[M+Na]+
472.3022@609.16 (M0)
473.3055@609.16 (13C/12C)
474.3085@609.16 (13C/12C*2)
[M+H-H2O]+
432.3098@609.16 (M0)
433.3132@609.16 (13C/12C)
434.3162@609.16 (13C/12C*2)
[M+H-2*(H2O)]+
414.2993@609.16 (M0)
415.3027@608.85 (13C/12C)
416.3054@609.16 (13C/12C*2)
e
[M+H]+
[M+Na]+
[M-H2O+H]+
[M-2H2O+H]+
M0
13C/12C
13C/12C*2
f
ESI+
ESI-
log10(Number)
Pre-annotated features
Unique khipus
HMDB Matched
g
ESI+
ESI-
HMDB Matched
No match

386

387

Figure 3: Most frequent neutral losses account for a small subset of LC-MS features.

a. Most frequence delta m/z values in positive ionization Orbitrap datasets.

b, **c**. The numbers and percentages of khipus and additional features explained by candidate fragments, in positive and negative ionization datasets, respectively.

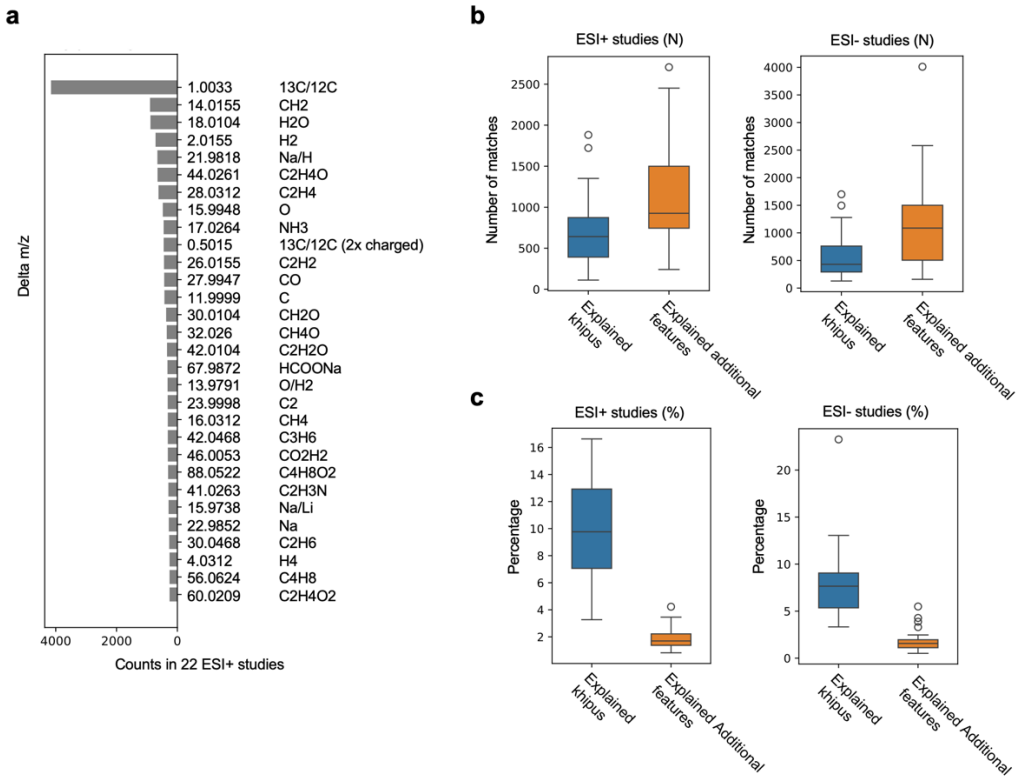

395 **Figure 4: MS/MS based search of ISFs.**
396

397 **a**. Example of matching MS/MS and MS spectra for searching ISFs. Top: MS/MS from MoNA.
398 Bottom: sample CHCL3_20min_B from dataset MTBLS1465_HILICpos__ppm5_3505731, MS
399 scan number 1408.

400 **b**. Absolute numbers of features matched to MoNA MS/MS spectra across the 45 LC-MS
401 studies, using positive and negative ionization respectively. In each boxplot, 1st column is the
402 number of features matching a precursor m/z value (P), the 2nd column the subset of P with
403 match to at least one MS/MS fragment (Y), and the 3rd column number of all matched MS/MS
404 fragments per study.

405 **c**. Conversion of **b** to percentages: P over total features (T), Y over T and Y over P.

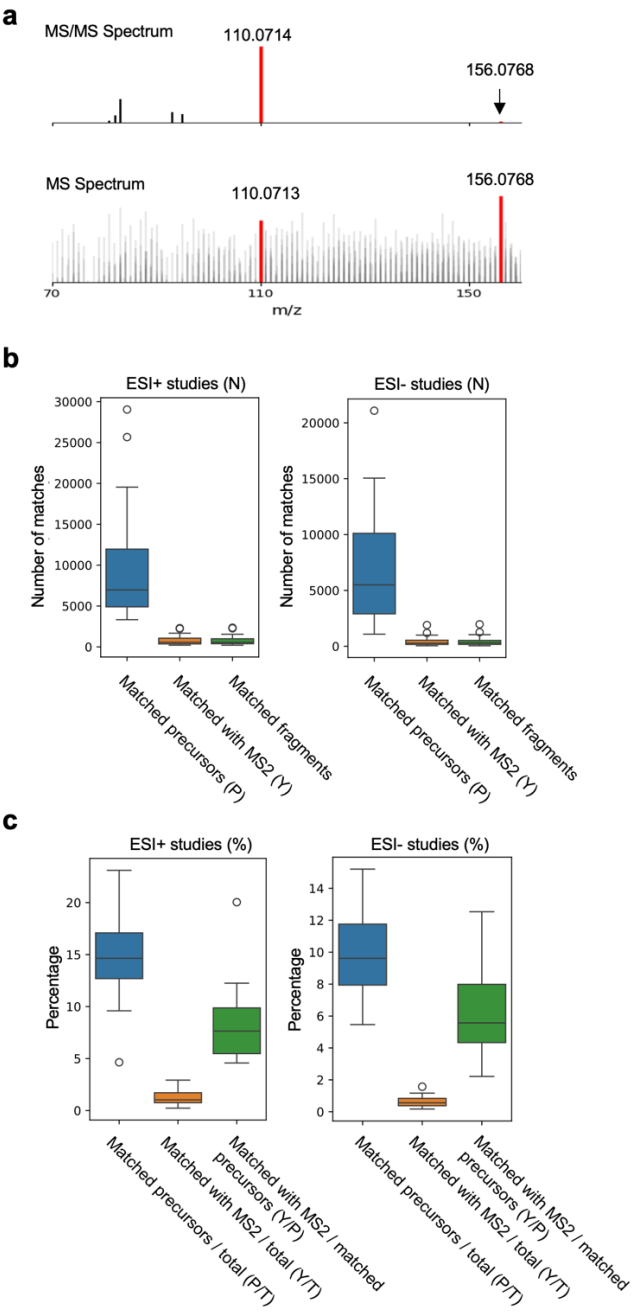
a
MS/MS Spectrum
110.0714
156.0768
MS Spectrum
110.0713
156.0768
70
110
150
m/z
b
ESI+ studies (N)
ESI- studies (N)
Number of matches
Matched precursors (P)
Matched with MS2 (Y)
Matched fragments
c
ESI+ studies (%)
ESI- studies (%)
Percentage
Matched precursors / total (P/T)
Matched with MS2 / total (Y/T)
Matched with MS2 / matched precursors (Y/P)

406

407

408 **Figure 5: Khipu based pre-annotation explains most of the abundant features.**

409 **a**. Top: Distribution of feature intensity in Figure 1c divided into quartiles, which are marked by
410 dashed lines.

411 Bottom: Percentage distribution of pre-annotated features in each intensity quartile cross
412 studies, shown as violin plots, for positive and negative ionization datasets respectively. The pie
413 charts show median percentage of contributions from M0, other isotopologues, in-source
414 fragments and singletons. Adducts are included in khipus, and singletons are the unexplained
415 features.

416 **b**. Abundance difference between [M0+H]+ features and singletons within the top quartile.
417 Example from study ST001237_HILICpos_B2_ppm5_3524314, p-value < 1E-25 by Student t-
418 test.

419 **c**. Percentage of pre-annotated features versus feature abundance quantile (1%-99% stepwise
420 by 1%) from 45 Orbitrap studies, for positive and negative ionization datasets respectively.

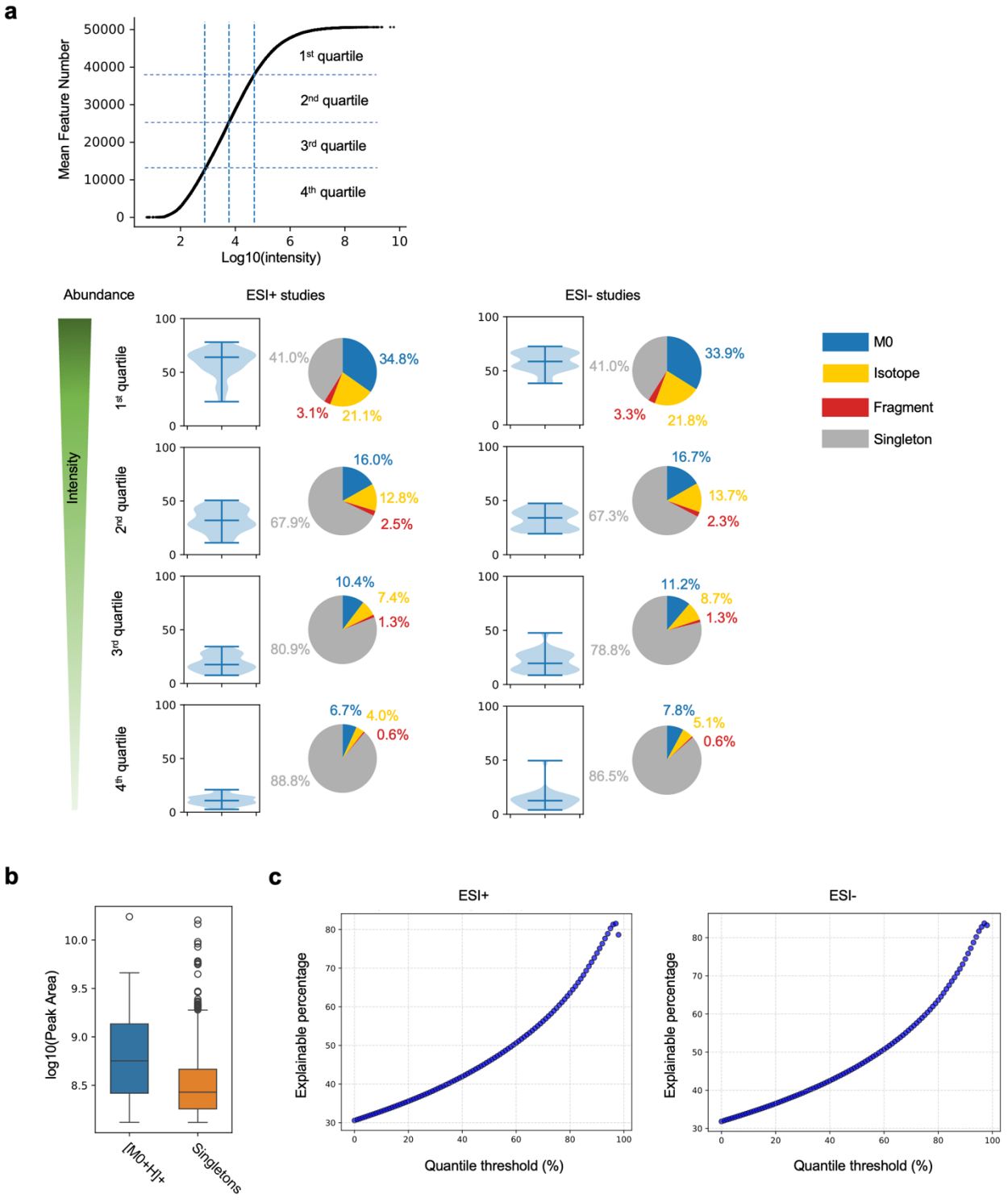
a
Mean Feature Number
Log10(intensity)
1st quartile
2nd quartile
3rd quartile
4th quartile
Abundance
ESI+ studies
ESI- studies
Intensity
1st quartile
2nd quartile
3rd quartile
4th quartile
41.0%
34.8%
3.1%
21.1%
67.9%
16.0%
12.8%
2.5%
80.9%
10.4%
7.4%
1.3%
88.8%
6.7%
4.0%
0.6%
41.0%
33.9%
3.3%
21.8%
67.3%
16.7%
13.7%
2.3%
78.8%
11.2%
8.7%
1.3%
86.5%
7.8%
5.1%
0.6%
M0
Isotope
Fragment
Singleton
b
log10(Peak Area)
[M0+H]+
Singletons
c
ESI+
ESI-
Explainable percentage
Quantile threshold (%)

421

422

Figure S1: Additional common mass differences and distribution of retention shift.

a. Most frequence delta m/z values in negative ionization Orbitrap datasets.

b. Example distribution of retention time shift (in seconds) associated with each delta m/z (labeled at top) in **Figure 3a**.

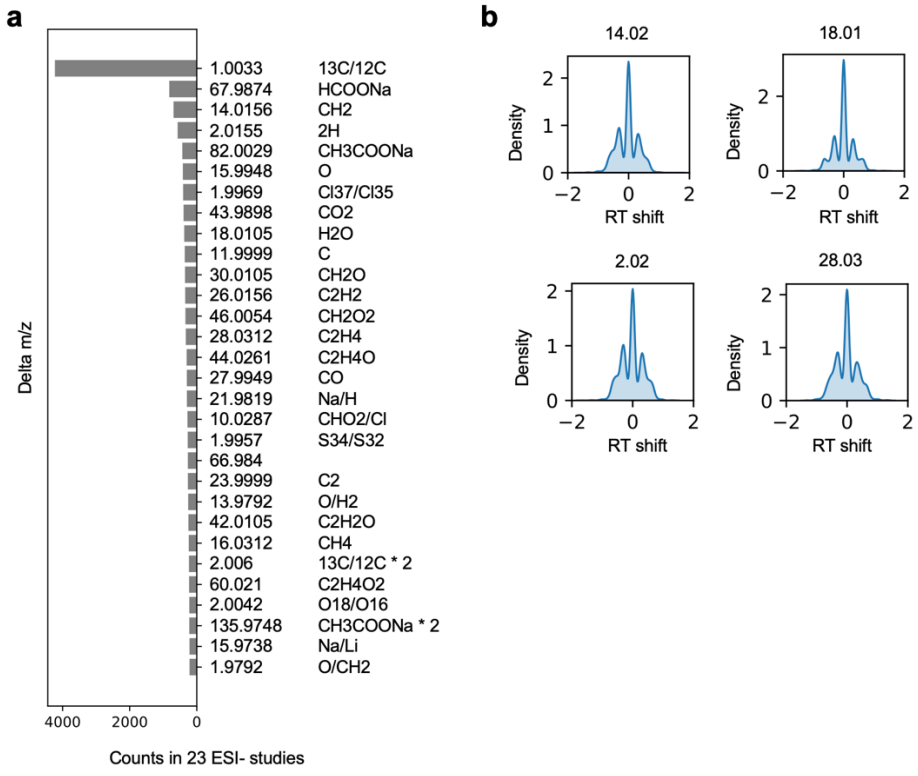

Methods

Data Retrieval and Processing

A total of 61 public, untargeted metabolomics studies were downloaded from Metabolomics Workbench (metabolomicsworkbench.org) and MetaboLights (www.ebi.ac.uk/metabolights/). All studies were based on human serum or plasma samples, totaling 3482 samples. Of the 61 total studies, 45 were collected using orbitrap-type mass analyzers and 16 using time-of-flight mass analyzers. The breakdown by chromatography and ionization type are noted in Table S1 but all permutations of HILIC, RP, ESI+ and ESI- were represented in all analyzer subsets. Large studies were down selected to between 100~120 samples.

The raw files were converted to centroided mzML files using ThermoRawFileParser v1.3.1 for Orbitrap data or msConvert v3 for ToF data. Data preprocessing was performed using Asari (v 1.13.1), yielding feature tables with m/z, retention time, peak shape, signal-to-noise ratio, chromatographic selectivity, detection count and intensity values per study. For all analyses, the full feature table was used which enforces the default feature quality filters (signal-to-noise ratio, or SNR, of 2, and a peak shape > 0.5 defined as goodness of fit to a gaussian model). Orbitrap studies were processed using the autoheight option enabled, while ToF data was processed using a mass accuracy of 25 ppm, a min_peak_height of 1000, a cal_min_peak_height as 3e4, and a min_intensity_threshold of 500. Mass calibration was performed according to the default parameters in Asari.

The MoNA MS/MS library were downloaded from https://mona.fiehnlab.ucdavis.edu/ (Feb 8, 2024) and the resulting spectra were deduplicated as follows using utilities from MatchMS (Huber2024). First all spectra for the same precursor inchikey were identified to yield a spectral cluster. Within each spectral cluster, in the second step, the pairwise cosine similarity is calculated for all pairs. The sum of the cosine similarity score weighted by the number of matched peaks for all such comparisons per spectrum is then calculated. Lastly, the spectrum with the largest sum score for that inchikey is then selected as the exemplar for that inchikey and all others are discarded. All collision energy spectra were considered during deduplication with the assumption that the most common fragments should be frequently shared across collision energies.

LC-MS analysis of glycochenodeoxycholic acid

463 The chemical standard of glycochenodeoxycholic acid (Cayman Chemical, catalog number 16942)
464 was prepared with acetonitrile at 1 µg/mL. The standard was run using a HILIC column on a
465 Thermo Scientific Q Exactive HF-X Mass Spectrometer (Thermo Fisher Scientific, MA, USA)
466 coupled to Thermo Scientific Transcen LX-2 Duo UHPLC system (Thermo Fisher Scientific, MA,
467 USA), with a HES-II ionization source. The HILIC method utilized an Accucore™ 150 Amide
468 column (10x2.1 mm guard; 100x2.1 mm analytical) with 10 mM ammonium acetate mobile phases
469 (95:5 acetonitrile:water, v/v) containing 0.1% acetic acid, with a gradient from 0% to 98% B2 over
470 20 minutes at a flow rate of 0.55 mL/min and 45 °C column temperature. MS data were acquired
471 in positive ionization modes (66.7–1000.0 m/z, resolution 60,000 at m/z 200) with optimized ion
472 source parameters, including 3.5 kV spray voltage, 300 °C capillary temperature, and 425 °C
473 heater temperature.
474
475 **Search of m/z patterns**
476 The isotopic pairs, $^{13}C/^{12}C$ features, are defined by annotation of matched retention time, mass
477 distance of 1.003355, and intensity of ^{13}C feature under 50% of that of ^{12}C feature. The RT
478 differences of all isotopic pairs in each dataset were calculated, and their standard deviation
479 was used to define the RT coelution window per study (one standard deviation on either side of
480 the molecular ion).
481
482 To compare MS/MS data to LC-MS data, our deduplicated MoNA MS/MS library is used (13973
483 precursors in positive and 9184 in negative). A 5-ppm mass tolerance was used for both
484 precursor and MS/MS peak matching with features in retention time window. Only MS/MS
485 peaks whose normalized intensity was higher than 0.1 was considered. To compare common
486 mass difference to LC-MS data, in-source fragment candidates are manually selected from
487 common mass differences, and the minimum of 5 ppm of m/z value or 0.0005 as absolute value
488 was used for mass delta matching. Results here are searched on the top 5 MS/MS fragments,
489 while using top 10 fragments led only to minor increase of matches (not shown).
490
491 **Calculation of common mass differences**
492 For the molecular ion in each khipu, the m/z differences to all other features in the elution
493 window were calculated and counted in a histogram (bin size 0.0001 for Orbitrap data, 0.0005
494 for TOF data). The histogram was smoothed, and peak values were selected by a threshold
495 (100 for Orbitrap data, 20 for TOF data). The top 20 mass differences (deltas) were selected per
496 ionization mode to be used as candidate in-source fragments.

Pre-annotation using Khipu

Khipu performs pre-annotation by assigning co-eluting features to adduct and isotopologue relations using a generic tree structure based on *a priori* mass delta patterns (Li2023a). The minimum of 5 ppm of m/z value or 0.0005 as absolute value was used for mass delta matching. The conservative parameters used in Figure 3 without ISFs are as follows: in positive ionization mode, isotope patterns 13C/12C at m/z 1.0034, 13C/12C × 2 at m/z 2.0067, and 37Cl/35Cl at m/z 1.9970; adducts Na/H at m/z 21.9819, ACN at m/z 41.0265, NaCOOH at m/z 67.9874, K/H at m/z 37.9559, and CH3OH at m/z 32.0262. In negative ionization mode, isotope patterns 13C/12C at m/z 1.0034, 13C/12C × 2 at m/z 2.0067, 37Cl/35Cl at m/z 1.9970, and 32S/34S at m/z 1.9958; adducts Na/H at m/z 21.9819, NaCOOH at m/z 67.9874, and NaCH2COOH at m/z 82.0030. The parameters for comprehensive khipu analysis in Figures 2 and 5 are given in Table S6.